Diffusion nuclear magnetic resonance spectroscopy detects substoichiometric concentrations of small molecules in protein samples

Ribeiro, João P.; Palczewska, Małgorzata; André, Sabine; Cañada, F. Javier; Gabius, Hans-Joachim; Jiménez-Barbero, Jesús; Mellström, Britt; Naranjo, José R.; Scheffers, Dirk-Jan; Groves, Patrick

Published in:
Analytical Biochemistry

DOI:
10.1016/j.ab.2009.09.001

Publication date:
2010

Analytical Biochemistry 396 (2010) 117–123

Contents lists available at ScienceDirect

Analytical Biochemistry

journal homepage: www.elsevier.com/locate/yabio

Diffusion nuclear magnetic resonance spectroscopy detects substoichiometric concentrations of small molecules in protein samples

João P. Ribeiro [a], Małgorzata Palczewska [b,c], Sabine André [d], F. Javier Cañada [a], Hans-Joachim Gabius [d], Jesús Jiménez-Barbero [a], Britt Mellström [c], José R. Naranjo [c], Dirk-Jan Scheffers [e], Patrick Groves [a,b,*]

[a] Chemical and Physical Biology, Centro de Investigaciones Biológicas, CSIC, 28040 Madrid, Spain
[b] Molecular Interactions and NMR Laboratory, Instituto de Tecnologia Química e Biológica, Universidade Nova de Lisboa, 2780-157 Oeiras, Portugal
[c] Department of Molecular and Cellular Biology, Centro Nacional de Biotecnología, CSIC, 28049 Madrid, Spain
[d] Institut für Physiologische Chemie, Tierärztliche Fakultät, Ludwig-Maximilians-Universität München, 80539 München, Germany
[e] Bacterial Membrane Proteomics Laboratory, Instituto de Tecnologia Química e Biológica, Universidade Nova de Lisboa, 2780-157 Oeiras, Portugal

ARTICLE INFO

Article history:
Received 23 July 2009
Available online 4 September 2009

Keywords:
Contamination
Diffusion
DOSY
Lectin
Protein purification
Relaxation

ABSTRACT

Small molecules are difficult to detect in protein solutions, whether they originate from elution during affinity chromatography (e.g., imidazole, lactose), buffer exchange (Tris), stabilizers (e.g., β-mercaptoethanol, glycerol), or excess labeling reagents (fluorescent reagents). Mass spectrometry and high-pressure liquid chromatography (HPLC) often require substantial efforts in optimization and sample manipulation to provide sufficient sensitivity and reliability for their detection. One-dimensional (1D) ^{1}H nuclear magnetic resonance (NMR) could, in principle, detect residual amounts of small molecules in protein solutions down to equimolecular concentrations with the protein. However, at lower concentrations, the NMR signals of the contaminants can be hidden in the background spectrum of the protein. As an alternative, the 1D diffusion difference protocol used here is feasible. It even improves the detection level, picking up NMR signals from small-molecule contaminants at lower concentrations than the protein itself. We successfully observed 30 μM imidazole in the presence of four different proteins (1–1.5 mg/ml, 6–66 kDa, 25–250 μM) by 1D diffusion-ordered spectroscopy (DOSY) difference and 1-h total acquisition time. Of note, imidazole was not detected in the corresponding 1D ^{1}H NMR spectra. This protocol can be adapted to different sample preparation procedures and NMR acquisition methods with minimal manipulation in either deuterated or nondeuterated buffers.

Proteins are prepared and purified by a wide variety of processes. Commonly, analyses of preparations focus on protein concentration and activity together with purity to assess the presence of any other proteins as a contamination. Of note, solutions can also contain low-molecular-weight compounds whose presence may affect protein properties and, thus, needs to be assessed. The presence of small molecules can compromise the quality of enzyme preparations, the accurate measurement of biophysical parameters for proteins, the ability of a given protein to crystallize, or formal approval for biomedical application. High-pressure liquid chromatography (HPLC[1]), capillary electrophoresis [1], and mass spectrometry [2] are sensitive methods to detect small-molecule contaminants. However, careful parameter optimization is essential to adapt them to the specific detection of distinct small molecules. Thus, it is prudent to develop efficient nondestructive assays to identify the presence of small molecules in protein-containing solutions that require no sample manipulations or optimization of conditions. Here we present a nuclear magnetic resonance (NMR)-based assay to address this issue.

Standard ^{1}H NMR spectroscopy, if time is available for the necessary accumulation of scans, facilitates the detection of micromolar concentrations of low-molecular-weight compounds (<1000 Da). However, it is inherently difficult to unambiguously distinguish these signals from the background of protein signals at equimolar ratios of the small molecule and the protein. NMR can exploit the different physical properties of small and large molecules, in particular those based on relaxation and diffusion. Diffusion-ordered spectroscopy (DOSY) separates the NMR spectra of molecules based on size [3–6]. Such methods are regularly used to filter out signals from low-molecular-weight substances, in particular as a solvent suppression method [7–9]. In addition, DOSY strategies have been implemented to detect and screen potential

* Corresponding author.
E-mail address: pgroves@itqb.unl.pt (P. Groves).

[1] *Abbreviations used:* HPLC, high-pressure liquid chromatography; NMR, nuclear magnetic resonance; DOSY, diffusion-ordered spectroscopy; 1D, one-dimensional; BSA, bovine serum albumin; CG-1B, chicken galectin 1B (formerly C-14); hgal-1, human galectin 1; 2D, two-dimensional; GDP, guanosine-5′-diphosphate; MWCO, molecular weight cutoff; DREAM, downstream regulatory element antagonist modulator; cDNA, complementary DNA; OD, optical density; UV, ultraviolet; EDTA, ethylenediaminetetraacetic acid; GraPES, gradient phase encoded spin-lock.

0003-2697/$ - see front matter © 2009 Elsevier Inc. All rights reserved.
doi:10.1016/j.ab.2009.09.001

interactions of proteins with low-molecular-weight ligands [10]. The combination of relaxation and diffusion strategies has been shown to be effective for the removal of protein and membrane constituent signals from plasma samples to obtain a refined spectrum of metabolites [11]. Similar combined strategies have also proven to be useful for the analysis of ligand-binding studies [12,13]. None of these combined methods has been applied to the issue of protein purity.

The current work is focused on the detection of small molecules, not necessarily binders/ligands, present in protein samples at residual or substoichiometric concentration after purification and/or sample preparation protocols that could contaminate and compromise further studies with the proteins. As a consequence, we record one one-dimensional (1D) DOSY spectrum under conditions where no resonances are filtered out and a second spectrum under conditions where the small-molecule resonances are deliberately filtered out. The difference spectrum is obtained by scaling the two spectra, resulting in a high-quality spectrum of any small molecules present in the solution. The protocol is of interest to all scientists who produce protein samples, and it uses a standard pulse program commonly distributed with Bruker instruments that could be easily implemented for other spectrometers.

Materials and methods

Materials

Aprotonin (product No. A1153), α-lactalbumin (product No. L6010), carbonic anhydrase (product No. C3934), bovine serum albumin (BSA, product No. A0281), imidazole, and sodium phosphate were purchased from Sigma–Aldrich (St. Louis, MO, USA) and used without further manipulation. The prototype chicken galectin 1B (CG-1B, formerly C-14) and human galectin 1 (hgal-1) were obtained by recombinant production, purified to homogeneity by affinity chromatography as a crucial step, and controlled for purity by 1D and two-dimensional (2D) gel electrophoresis, gel filtration, and electrospray ionization mass spectrometry as well as for activity by solid-phase and cell assays [14–18]. Lectin-containing solutions in phosphate buffer were lyophilized. *Bacillus subtilis* FtsZ was expressed and purified as described previously [19,20]. Purified FtsZ was incubated on ice for 10 min with 1 mM guanosine-5′-diphosphate (GDP) and centrifuged to remove insoluble protein (30 min, 98,600*g*, 4 °C) and subsequently dialyzed in a 0.25-ml unit with 4-kDa molecular weight cutoff (MWCO, G Biosciences, Maryland Heights, MO, USA) against two changes of 10 mM Tris–HCl and 50 mM KCl (pH 8.0) (2 L, 40 h) and against two changes of 10 mM Tris–d11, 50 mM KCl (pH 7.7), and 99% ^2H_2O (15 ml, 12 h). Samples were prepared in NE-HL5 NMR tubes, and an NE-5-CIC coaxial insert was used in the indicated experiments (New Era via Cortec, Paris, France). Deuterated materials (^2H_2O and Tris–d11) were purchased from Cambridge Isotope Laboratories (Andover, MA, USA).

Protein expression and purification of DREAM 71–256 and ubiquitin

Part of the human DREAM (downstream regulatory element antagonist modulator) complementary DNA (cDNA) coding region covering amino acids 71–256 was inserted between the *Nco*I/*Xho*I sites of the pET28a vector, resulting in expression of His-tagged DREAM 71–256. The DNA for His-tagged ubiquitin was synthesized and optimized for codon use in *Escherichia coli* (NZYtech, Lisbon, Portugal) and was cloned into the pET28 vector as above. Protein expression was performed in BL21(DE) cells (NZYtech), and protein purification was performed according to standard protocols. The expression of His-tagged proteins was induced with 0.5 mM isopropyl β-d-1-thiogalactopyranoside in bacteria grown to an optical density (OD) of 0.8, with bacteria thereafter allowed to grow for 3 h at 30 °C. Cells were collected by brief centrifugation and lysed in binding buffer (50 mM phosphate buffer [pH 7.0] and 300 mM NaCl) supplemented with protein inhibitors, 2.5 μg/ml DNase I, and 0.75 mg/ml lysozyme. After lysis, the protein extract was centrifuged again to separate the cell debris from soluble protein. The obtained extract was applied to a cobalt-loaded, chelating Sepharose Fast Flow column (GE Healthcare, Uppsala, Sweden). The resulting fractions containing pure protein according to polyacrylamide gel electrophoresis were pooled and dialyzed extensively in a 2.5-ml, 4-kDa MWCO unit (G Biosciences) against 800 ml of dialysis buffer (10 mM phosphate and 100 mM NaCl [pH 6.8] for DREAM 71–256 and 0.5× phosphate-buffered saline for ubiquitin) with five changes each 8–16 h. The final protein concentrations were determined with Roti-NanoQuant (Carl Roth, Karlsruhe, Germany) according to the manufacturer's protocol and by ultraviolet (UV) absorption (calculated $\varepsilon = 22{,}000\ \text{mol cm}^{-1}$ at 280 nm for DREAM and $\varepsilon = 1490\ \text{mol cm}^{-1}$ at 280 nm for ubiquitin) as 2.0 ± 0.1 mg/ml (80 μM, DREAM) and 1.5 ± 0.3 mg/ml (160 μM, ubiquitin). The dialyzed solutions of DREAM were diluted twofold with ^2H_2O in preparation for NMR measurements. Ubiquitin samples consisted of 400 μl of H_2O sample with 10 μl of ^2H_2O added for the field frequency lock.

NMR spectroscopy

Spectra were recorded on a Bruker Avance III 500-MHz instrument running TopSpin 2.1 equipped with a triple resonance TXI probe and on a Bruker Avance II 600-MHz instrument running XWIN-NMR equipped with a TXI cryoprobe. The p3919gp pulse program was used to obtain 1D ^1H NMR data, the stimulated echo stebpgp1s19 pulse program was used for 2D DOSY spectra, and the stebpgp1s191d and stebpgp1s1d pulse programs were used for 1D DOSY spectra with and without Watergate solvent suppression, respectively. Spectral widths of 40 ppm were set to facilitate automatic baseline correction. Values of Δ, δ, and NS are indicated in the text and figure legends. For 1D DOSY difference, Δ = 100 ms, δ = 1 ms, and NS = 1024 were routinely applied parameters with two spectra collected with gradient strengths of GPZ6 = 0% and GPZ6 = 100% (effectively 0 and ∼35 G/cm for the shaped gradients used in the pulse sequences) that were found to be optimal on the 500-MHz instrument. The two 1D DOSY spectra were processed, phased, and baseline corrected with identical parameters. Phase distortion of the peaks and a skewed baseline close to the residual water signal, particularly in the GPZ6 = 0% spectrum, were reduced by applying a digital filter according to Marion and coworkers [21] at a cost of losing the intensity of some signals close to the water resonance. The 100% spectrum was overlaid onto the corresponding 0% spectrum. The 100% spectrum was scaled up by approximately 100% until the visible protein signals matched, and then the difference was calculated and stored. The positive peaks in the difference spectrum are assigned to small molecules present in the protein solution. The 2D DOSY spectra were processed in the corresponding two dimensions, chemical shifts (δ, ppm) in abscissas and translational diffusion coefficients (D, $\text{m}^2\ \text{s}^{-1}$) in ordinates, with the DOSY module provided with the XWIN-NMR/TopSpin software.

Results

Initial evidence for the described method emerged during the analysis of the oligomeric state of adhesion/growth–regulatory lectins (galectins) [22,23] by 2D DOSY methods and studying the effect of oligosaccharide ligands on the lectins' quaternary

structure. The lectins were purified by affinity chromatography, and lactose was routinely used to release the protein from the ligand-bearing resin [24]. The next step involved extensive dialysis to remove lactose from the protein samples. The absence of characteristic lactose resonances in the 3- to 4-ppm region of the 1D ^{1}H NMR spectrum appears to confirm that this molecule has been completely removed from a solution containing CG-1B (Fig. 1A). On inspecting the 2D DOSY spectrum of the same CG-1B-containing sample, a series of small deflections became detectable toward faster diffusion in the 3- to 4-ppm range (Fig. 1B). The diffusion dimension is processed by fitting an equation that calculates the average diffusion coefficient at each position of the chemical shift. For a pure protein, we would expect to see a straight line across the whole spectrum because the diffusion coefficient is a property of the entire molecule. The downward deflections observed in Fig. 1B are characteristic of overlapping resonances from small, fast-diffusing molecules such as β-mercaptoethanol and Tris. However, the broader series of downward deflections in the 3- to 4-ppm region is not characteristic for a simple small molecule that contains one or two sharp resonances. In contrast, it is attributable to the presence of lactose ^{1}H NMR resonances (Fig. 1C). Evidently, the 2D DOSY experiment detected a small quantity of free lactose in the protein solution that was not tracked down in the 1D ^{1}H NMR spectrum. This conclusion, however, is based on our experience of acquiring DOSY data over the years and is not entirely unambiguous. To solidify the inferred concept, we set out to develop a robust and objective protocol (a concise version is available in the Supplementary material).

Routine 2D DOSY experiments comprise a series of 32 experiments over a gradient range. The change in signal intensity for three types of molecules with different sizes over the applied gradient range is simulated in Fig. 2. The first experiment (Fig. 2, gradient = 0 G/cm) involves very little signal filtering and essentially corresponds to a normal 1D ^{1}H spectrum. As ensuing experiments are run, the gradient pulse providing the diffusion filtering is gradually increased and the signals from small molecules decay more rapidly, according to Eq. (1):

$$\ln I/I_o = -D(2/\pi)^2 G^2 \gamma^2 \delta^2 (\Delta - \delta/4), \quad (1)$$

where I is the intensity, I_o is the intensity when $G = 0$ G/cm, D is the diffusion coefficient (cm^2 s^{-1}), G is the strength of the applied gradient (G/cm), γ is the proton gyromagnetic ratio, δ is the time (s) that the gradient field pulse is active, and Δ is the time (s) between gradient pulses to allow diffusion of the molecules.

The shape of the signal decay for each molecule is the same for each resonance, although the accuracy of the fitting will depend on the relative intensity of the different resonances. For a good-quality DOSY spectrum, we aim at reducing the intensity of our protein signals (Fig. 2, squares) by more than 90% when we apply the maximum gradient strength in the final experiment (Fig. 2, gradient = 35 G/cm). Under the same conditions, the signals of small molecules are generally reduced by more than 99% by the middle of the experiment compared with a reduction of approximately 50% for the protein (Fig. 2, triangles, gradient ~14 G/cm). Acquisition of a 1D DOSY spectrum corresponding to the middle gradient increment of the 2D DOSY series results in a representative 1D ^{1}H spectrum of the protein where intensities of the signals of small molecules have been greatly reduced relative to those of the protein; this is a well-established method to suppress solvent resonances (Fig. 2, circles) [7–9]. Our aim to reliably pick up signals from small molecules can be achieved by the comparison of 1D DOSY spectra corresponding to the first and middle spectra in the 2D DOSY. The 1D DOSY difference spectrum enables an objective interpretation in contrast to the subjective interpretation of the deflections present in the 2D DOSY spectrum (Fig. 1B). An additional advantage of collecting 1D spectra over 2D spectra is a saving of time or, alternatively, increasing the signal/noise ratio by performing more scans per experiment.

Fig. 2 suggests that the optimal gradient strengths in 1D DOSY experiments to differentiate between a low-molecular-weight molecule (e.g., Tris) and a protein (e.g., the homodimeric hgal-1) are gradient strengths of 0 and 14 G/cm. However, it is desirable to use the shortest possible values of Δ and δ in the DOSY experiment to minimize relaxation losses during the diffusion delay, Δ. Gradient strengths of 0 and 35 G/cm with $\Delta = 100$ ms and

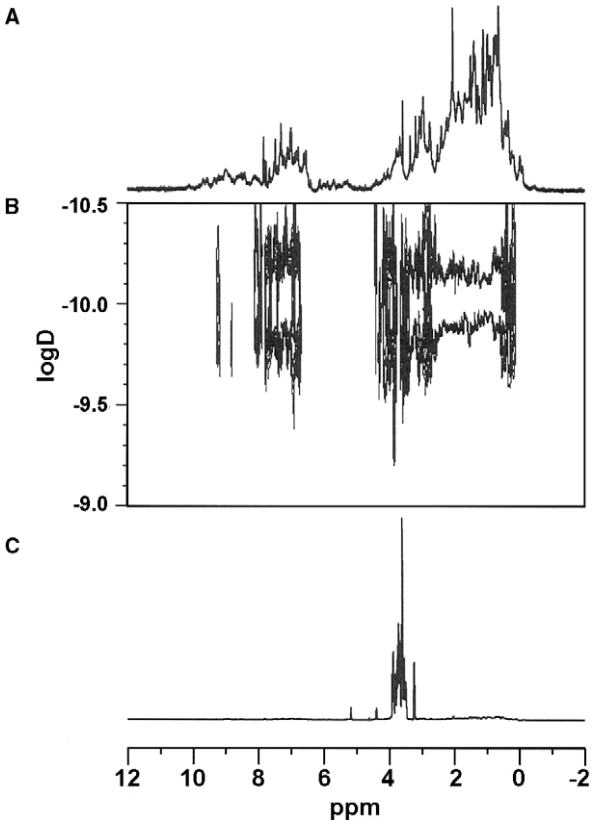

Fig. 1. NMR analysis of CG-1B. (A) 1D ^{1}H NMR spectrum of CG-1B. (B) 2D DOSY spectrum of CG-1B. (C) 1D ^{1}H NMR spectrum of lactose.

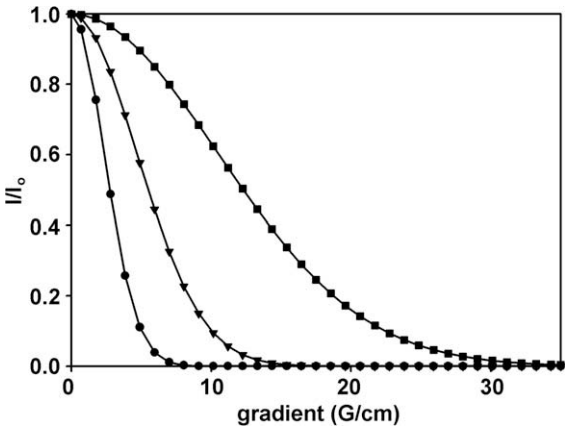

Fig. 2. Simulated plots of relative intensity versus gradient strength for three different molecules. The traces are for water (●, $D = 2 \times 10^{-9}$ m^2 s^{-1}), a small molecule of 100–200 Da (▼, $D = 5 \times 10^{-10}$ m^2 s^{-1}), and an approximately 30-kDa protein (■, $D = 1 \times 10^{-10}$ m^2 s^{-1}). Values of $\Delta = 0.4$ s and $\delta = 4$ ms were used for the simulation.

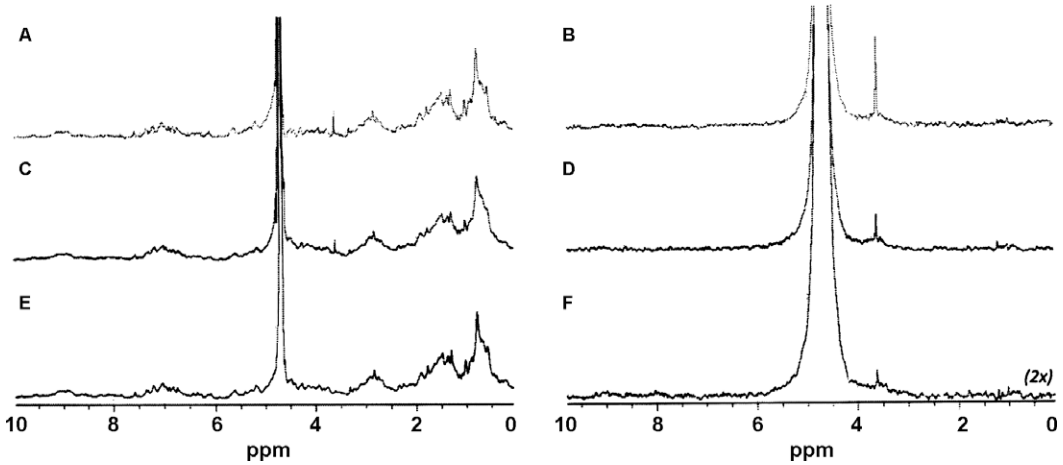

Fig. 3. 1D ^{1}H (left panels) and 1D DOSY difference (right panels) spectra of samples of hgal-1 at a concentration of 110 μM: (A, B) after adding 20 μM Tris; (C, D) after adding 5 μM Tris; (E, F) after adding 1 μM Tris. The 1D DOSY difference spectra were recorded with the stebpgp1s1d sequence and no solvent suppression. All 1D ^{1}H spectra were acquired over 16 scans, and the 1D DOSY difference spectra were acquired over 2 × 1024 scans (~1 h, panels B and D) and 2 × 2048 scans (~2 h, panel F).

δ = 1 ms were found to be optimal for our equipment (we use Δ = 400 ms and δ = 4 ms for protein analyses and the simulation in Fig. 2). These modified conditions were used in 1D DOSY experiments on samples of hgal-1 supplemented with low concentrations of Tris buffer to simulate a buffer exchange scenario. 1D DOSY provided detection of 1 μM Tris on a 600-MHz spectrometer fitted with a cryoprobe (Fig. 3), whereas 1D ^{1}H NMR experiments failed to detect the presence of Tris. These samples were prepared in deuterated buffer, and the experiments were performed without applying solvent suppression.

Next, we tested the detection limit of the 1D DOSY difference method in samples prepared in standard buffers (simply containing minimal concentrations of $^{2}H_2O$ to maintain the lock signal) by adding imidazole to four proteins of different molecular weights (Fig. 4). Aprotonin (6.6 kDa) produces very sharp resonances. As a result, signals of imidazole can readily be hidden within the

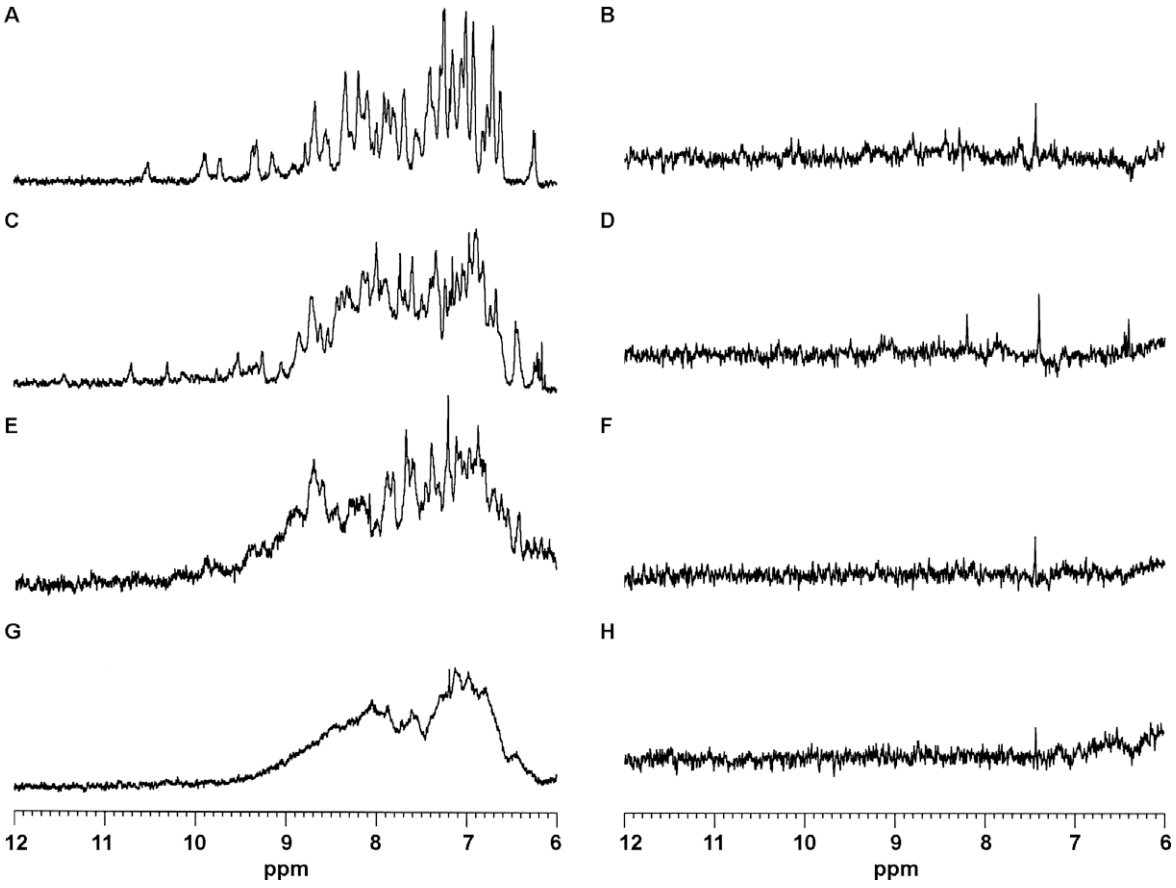

Fig. 4. 1D ^{1}H (left panels) and 1D DOSY difference (right panels) spectra of four protein standards with 30 μM imidazole added: (A, B) aprotonin (6.6 kDa); (C, D) α-lactalbumin (14.4 kDa); (E, F) carbonic anhydrase (30 kDa); (G, H) BSA (66 kDa). The 1D ^{1}H spectra were recorded in a 256-scan experiment (6 min), and the 1D DOSY difference is the result of two 1024-scan experiments (54 min). The imidazole signals appear at 7.4 and 8.2 ppm. For clarity, only the low-field signals are shown.

protein resonances. In contrast, the spectrum of BSA (66 kDa) has very broad resonances from which the sharp imidazole resonances may prove to be visible in 1D ^{1}H NMR spectra without resorting to the 1D DOSY difference method. The other proteins tested were α-lactalbumin (14.4 kDa) and carbonic anhydrase (29 kDa) of intermediate size and properties. Overall, we found that the results for all four proteins were similar. Two 1D DOSY spectra were obtained with a total accumulation time of 54 min, and a detection level of 30 μM imidazole was apparent for each of these proteins (Fig. 4), based on titrations of 0, 10 20, 30, and 40 μM imidazole. For comparison, the peaks for 30 μM imidazole could not be clearly identified in the 1D ^{1}H NMR spectra of any of these samples (Fig. 4).

One reason for concern regarding the spectra presented so far is that the samples contain 5–100% ^2H_2O. This represents a source of sample contamination and/or manipulation to prepare the NMR samples. The α-lactalbumin samples shown in Fig. 4C and D were dissolved in 100% H_2O solutions, and the ^2H_2O necessary for the lock was presented in a coaxial insert. The insert did not compromise the detection limits of the 1D DOSY difference experiment (Fig. 4).

Standard 1D ^{1}H NMR spectra are already useful when the small molecule is in excess over the protein. For example, Fig. 5A and C, and (to a lesser extent) 5E readily illustrate the presence of imidazole during the early stages of dialysis of His-tagged ubiquitin. The imidazole peaks can be assigned with certainty by 1D ^{1}H DOSY difference (Fig. 5H) while being undetectable by 1D ^{1}H NMR (Fig. 5G) for the same sample. To broaden the experimental basis, the 1D DOSY difference spectra methodology was applied to two other protein samples. DREAM is a calcium-binding protein with unique DNA-regulating properties within the EF-hand family [25]. His-tagged DREAM 71–256 was dialyzed after elution using 150 mM imidazole. It forms an oligomeric molten globule structure [26], and no sharp resonances are observed in its 1D ^{1}H NMR spectrum. After the last dialysis step (Fig. 5K and L), imidazole was detectable in neither the 1D ^{1}H NMR DOSY nor the 1D DOSY, meaning that imidazole, if present, should be below a concentration level of 30 μM. FtsZ (40.2 kDa) is the bacterial homologue of tubulin [19,27]. FtsZ was dialyzed from a 10% glycerol stock solution; commonly, glycerol is not easily removed by dialysis (Fig. 5M and N). The sharp resonance at 3.7 ppm is due to the residual ^{1}H signal from the deuterated Tris buffer. Rather small peaks in the 3- to 4-ppm region originate from residual glycerol and ethylenediaminetetraacetic acid (EDTA). For comparison, only the residual Tris signal was detected in the 1D ^{1}H NMR spectrum.

Discussion

It was our aim to present a facile NMR protocol for tracking down the presence of small molecules in protein samples. After the optimization of several parameters for the 1D ^{1}H DOSY pulse program (see Materials and methods and Supplementary material for details), we were able to detect substoichiometric concentrations of small molecules in protein samples. To underscore a general applicability, we tested a range of defined samples as well as chromatography eluates and their dialysates. Therefore, the presented NMR spectroscopy approach is revealed as a valuable tool for assessing the level of low-molecular-weight compounds in protein preparations at concentrations typically found in fractions obtained by elution during affinity chromatography (∼1 mg/ml, ⩾10 μM). The method is of interest to protein crystallographers as well as to those involved in a range of biochemical and pharmaceutical applications. 1D ^{1}H NMR spectra, due to the large differences in transversal relaxation between low-molecular-weight compounds (<1 kDa) and high-molecular-weight compounds (>10 kDa), can readily detect small molecules despite the broad protein resonances when their concentration is higher than that of the protein. As added value, 1D ^{1}H DOSY difference complements the standard 1D ^{1}H NMR experiment when the sample contains small proteins (<100 kDa) with defined resonances or when the contaminants are present in a quantity below the protein concentration. One could envision 1D ^{1}H difference spectra to improve the detection limit for small molecules. However, this approach requires the availability of the spectrum of a pure protein collected under identical sample and spectrometer conditions. Because this is difficult to attain, any positive result will be subject to a degree of uncertainty. Clearly, an advantage of the 1D DOSY difference method is that it does not rely on a reference sample.

An inherent limitation of the 1D ^{1}H NMR and 1D DOSY methods is that the low-molecular-weight ligand or contaminant must contain nonexchangeable ^{1}H signals (inorganic salts such as phosphate are not directly observable by ^{1}H NMR). A second limitation is that only free small molecules will be detected; any protein-associated compound will share the same diffusion parameters of the protein. Regarding equipment, our work was carried out on Bruker 500- and 600-MHz instruments. Because the objective of 1D DOSY difference is to trace small molecules, it is likely that lower field strengths and analytical instruments used by chemists may be sufficient for this purpose, although detection limits might be compromised. Of note, we deliberately use a widely available pulse program from the Bruker pulse sequence library to illustrate applicability, acknowledging the possibility that other pulse sequences/programs may provide spectra with improved signal/noise ratio and detection limits for small molecules. The GraPES (gradient phase encoded spin-lock) pulse sequence incorporates a spin-lock to selectively remove protein signals so as to provide improved discrimination between protein and small-molecule signals [13]. However, resonances from highly mobile loops of proteins or post-translational modifications (i.e., in glycoproteins) may still appear to mimic small-molecule signals [13]. Therefore, the use of the GraPES pulse sequence in our protocol should provide two spectra with a mildly reduced signal/noise ratio for small molecules (26% reduction for the example in Ref. [13]) and a greatly reduced protein background. Residual protein resonances will be observed at both high and low diffusion gradient strengths, whereas small-molecule signals will be observed at only low diffusion gradient strength. A control titration of imidazole into pure buffer, using the stebpgp1s191d pulse program and the same parameters as for the spectra shown in Fig. 4, yielded a detection limit of 10 μM as compared with 30 μM in the presence of 1 mg/ml protein due to the complete absence of protein signals in this sample. Therefore, a two- to threefold improvement in the detection limit can be expected for the GraPES pulse sequences and other sequences that are as yet unavailable in distributed pulse program libraries. Finally, we have not collected data with equipment from other NMR spectrometer manufacturers (e.g., Varian, Jeol) and the pulse sequences/programs available to users of these instruments. However, the protocol described here should also be easily applicable to these instruments.

With our Bruker instruments, the detection limits are approximately 5–100 μM by 1D ^{1}H NMR spectroscopy, depending on the protein line widths, and 1–30 μM by 1D DOSY difference. The improvement in the detection levels of the 1D DOSY difference method is demonstrated in the test experiments with proteins of different molecular weights (Fig. 4), reaching a limit of less than 30 μM imidazole in 1 h. At this stage, it should be noted that 1D DOSY difference spectra are useful to qualitatively detect the presence of contaminants over a concentration offset of approximately 10–30 μM ^{1}H equivalents. However, we have not fully implemented DOSY to perform quantitative measurements of concentrations. Although resonances of equal peak volume from two

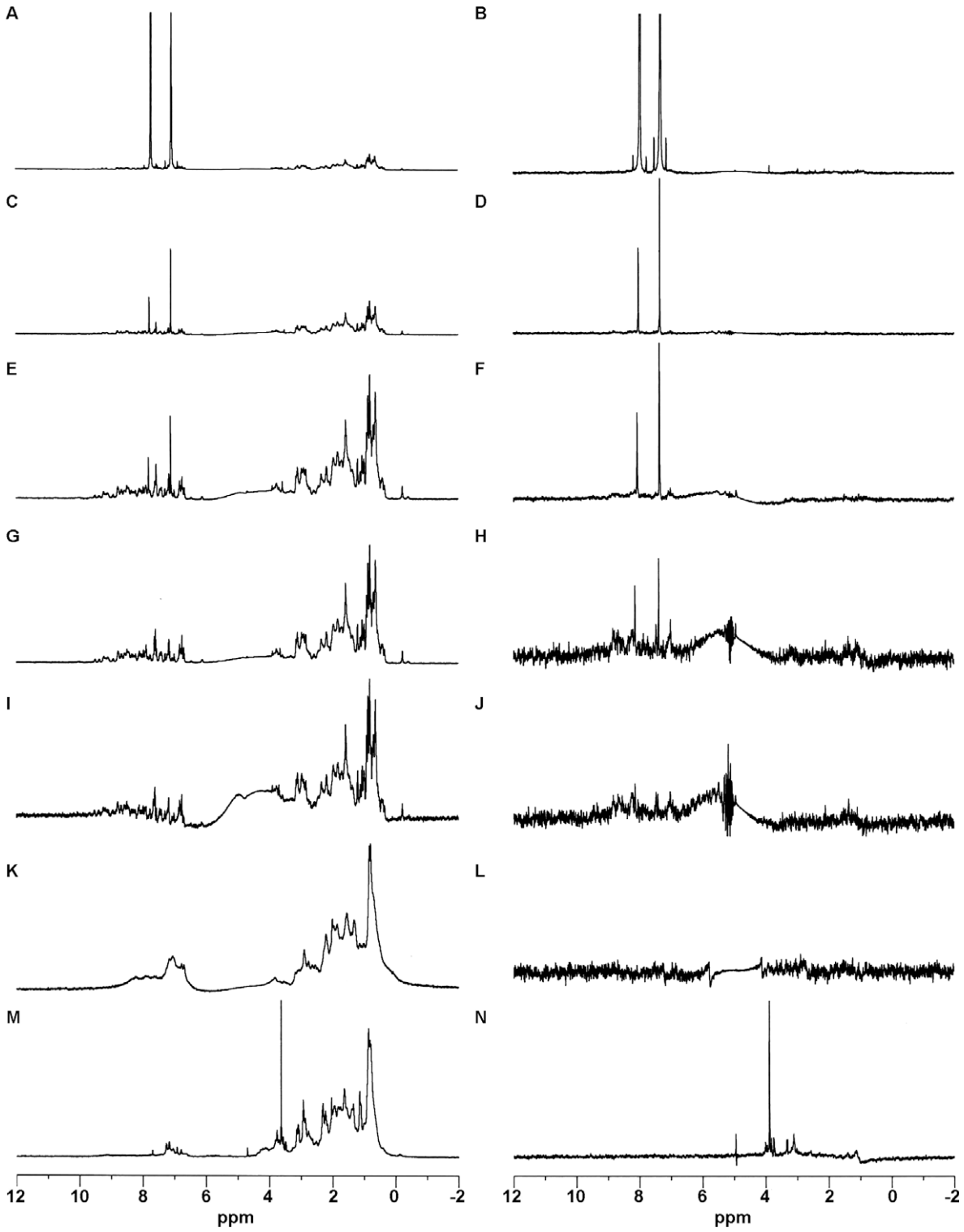

Fig. 5. 1D ^{1}H spectra (left panels) and 1D DOSY difference (right panels). (A, B) His-tagged ubiquitin eluted with buffer containing 150 mM imidazole. (C, D) His-tagged ubiquitin after one step of dialysis. (E, F) His-tagged ubiquitin after the second step of dialysis. (G, H) His-tagged ubiquitin after the third step of dialysis. (I, J) His-tagged ubiquitin after the fourth step of dialysis. (K, L) Present the final spectra obtained for His-tagged DREAM 71–256 after extensive dialysis. (M, N) Document spectra of FtsZ after dialysis and buffer exchange. The sharp peak at 3.9 ppm (both spectra) stems from residual protons in Tris–d11, and rather small peaks visible only in the 3- to 4-ppm section of the 1D DOSY difference spectrum arise from glycerol and EDTA. All experiments were run at parameters identical to those given in the legend to Fig. 4.

different molecules in a 1D ^{1}H NMR experiment indicate equivalent concentrations, this is not the case in the 1D DOSY difference spectrum because relative diffusion properties need to be considered. To establish a quantitative protocol, we suggest the titration of the small ligand into a solution of a pure protein at a concentration similar to that of the unknown samples (the pure protein of interest or a control protein of similar size). This titration can be used as a calibration to determine the concentration of small molecules. The expected errors for such a quantitative analysis are expected to be high, and the process is time-consuming for a single analysis. However, this approach may be valuable with respect to routine quality control in a process environment. In summary,

1D DOSY difference has been introduced as a method to detect the presence of subequimolar concentrations of small-molecule contaminants in protein samples.

Acknowledgments

We are grateful to Sara Fernandes, who helped to prepare the His-tagged ubiquitin samples. D.-J.S. and P.G. acknowledge the financial support of their groups from the Instituto de Tecnologia Química e Biológica (ITQB). J.P.R., S.A., H.-J.G., and J.J.-B. acknowledge generous funding from an EC Marie Curie Research Training Network grant (MRTN-CT-2005-019561). The Madrid group also thanks the Ministry of Science of Innovation of Spain (CTQ2006-10874-C02-01 and CTQ2009-8536). The 500-MHz NMR spectrometer used in this study is part of the Portuguese National NMR Network acquired with funds from Fundação para a Ciência e a Tecnologia (Portugal) and Fundo Europeo de Desenvolvimento Regional (FEDER).

Appendix A. Supplementary data

Supplementary data associated with this article can be found, in the online version, at doi:10.1016/j.ab.2009.09.001.

References

[1] K. Altria, A. Marsh, C. Sänger-van de Griend, Capillary electrophoresis for the analysis of small-molecule pharmaceuticals, Electrophoresis 27 (2006) 2263–2282.
[2] Y. Jiang, P.C. Wang, L.E. Locascio, C.S. Lee, Integrated plastic microfluidic devices with ESI-MS for drug screening and residue analysis, Anal. Chem. 73 (2001) 2048–2053.
[3] P. Stilbs, Molecular self-diffusion coefficients in Fourier transform nuclear magnetic resonance spectrometric analysis of complex mixtures, Anal. Chem. 53 (1981) 2135–2137.
[4] C.S. Johnson Jr., Diffusion ordered NMR spectroscopy: principles and applications, Prog. NMR Spectrosc. 34 (1999) 203–256.
[5] J.C. Cobas, P. Groves, M. Martín-Pastor, A. De Capua, New applications, processing methods, and pulse sequences using diffusion NMR, Curr. Anal. Chem. 1 (2005) 289–305.
[6] P. Groves, M. Palczewska, M.D. Molero, G. Batta, F.J. Cañada, J. Jiménez-Barbero, Protein molecular weight standards can compensate systematic errors in diffusion ordered spectroscopy, Anal. Biochem. 331 (2004) 395–397.
[7] M.L. Liu, J.K. Nicholson, J.C. London, High-resolution diffusion and relaxation edited one- and two-dimensional ^{1}H NMR spectroscopy of biological fluids, Anal. Chem. 68 (1996) 3370–3376.
[8] N. Esturau, J.F. Espinosa, Optimization of diffusion-filtered NMR experiments for selective suppression of residual nondeuterated solvent and water signals from ^{1}H NMR spectra of organic compounds, J. Org. Chem. 71 (2006) 4103–4110.
[9] M. Politi, P. Groves, M.I. Chávez, F.J. Cañada, J. Jiménez-Barbero, Useful applications of DOSY experiments for the study of mushroom polysaccharides, Carbohydr. Res. 341 (2006) 84–89.
[10] T. Brand, E.J. Cabrita, S. Berger, Intermolecular interaction as investigated by NOE and diffusion studies, Prog. NMR Spectrosc. 46 (2005) 159–196.
[11] M. Liu, J.K. Nicholson, J.C. Lindon, High-resolution diffusion and relaxation edited one- and two-dimensional ^{1}H NMR spectroscopy of biological fluids, Anal. Chem. 68 (1996) 3370–3376.
[12] W.H. Otto, C.K. Larive, Improved spin-echo-edited NMR diffusion measurements, J. Magn. Reson. 153 (2001) 273–276.
[13] B.A. Becker, K.F. Morris, C.K. Larive, An improved method for suppressing protein background in PFG NMR experiments to determine ligand diffusion coefficients in the presence of receptor, J. Magn. Reson. 181 (2006) 327–330.
[14] M.F. López-Lucendo, D. Solís, S. André, J. Hirabayashi, K.-I. Kasai, H. Kaltner, H.-J. Gabius, A. Romero, Growth–regulatory human galectin-1: crystallographic characterization of the structural changes induced by single-site mutations and their impact on the thermodynamics of ligand binding, J. Mol. Biol. 343 (2004) 957–970.
[15] S. André, Z. Pei, H.-C. Siebert, O. Ramström, H.-J. Gabius, Glycosyldisulfides from dynamic combinatorial libraries as *O*-glycoside mimetics for plant and endogenous lectins: their reactivities in solid-phase and cell assays and conformational analysis by molecular dynamics simulations, Bioorg. Med. Chem. 14 (2006) 6314–6326.
[16] H. Kaltner, D. Solís, J. Kopitz, M. Lensch, M. Lohr, J.C. Manning, M. Mürnseer, M. Schnölzer, S. André, J.L. Sáiz, H.-J. Gabius, Prototype chicken galectins revisited: characterization of a third protein with distinctive hydrodynamic behaviour and expression pattern in organs of adult animals, Biochem. J. 409 (2008) 591–599.
[17] M.F. López-Lucendo, D. Solís, J.L. Sáiz, H. Kaltner, R. Russwurm, S. André, H.-J. Gabius, A. Romero, Homodimeric chicken galectin CG-1B (C-14): crystal structure and detection of unique redox-dependent shape changes involving inter- and intrasubunit disulfide bridges by gel filtration, ultracentrifugation, site-directed mutagenesis, and peptide mass fingerprinting, J. Mol. Biol. 386 (2009) 366–378.
[18] S. André, H. Kaltner, M. Lensch, R. Russwurm, H.-C. Siebert, C. Fallsehr, E. Tajkhorschid, A.J.R. Heck, M. von Knebel-Doeberitz, H.-J. Gabius, J. Kopitz, Determination of structural and functional overlap/divergence of five prototype galectins by analysis of the growth–regulatory interaction with ganglioside GM1 in silico and in vitro on human neuroblastoma cells, Int. J. Cancer 114 (2005) 46–57.
[19] D.J. Scheffers, The effect of MinC on FtsZ polymerization is pH dependent and can be counteracted by ZapA, FEBS Lett. 582 (2008) 2601–2608.
[20] J. Löwe, L.A. Amos, Evolution of cytomotive filaments: the cytoskeleton from prokaryotes to eukaryotes, Int. J. Biochem. Cell Biol. 41 (2009) 323–329.
[21] D. Marion, M. Ikura, A. Bax, Improved solvent suppression in one-dimensional and two-dimensional NMR spectra by convolution of time-domain data, J. Magn. Reson. 84 (1989) 425–430.
[22] H.-J. Gabius, H.-C. Siebert, S. André, J. Jiménez-Barbero, H. Rüdiger, Chemical biology of the sugar code, ChemBioChem 5 (2004) 740–764.
[23] H.-J. Gabius (Ed.), The Sugar Code: Fundamentals of Glycosciences, Wiley–VCH, Weinheim, Germany, 2009.
[24] H.-J. Gabius, Influence of type of linkage and spacer on the interaction of β-galactoside-binding proteins with immobilized affinity ligands, Anal. Biochem. 189 (1990) 91–94.
[25] A.M. Carrión, W.A. Link, F. Ledo, B. Mellström, J.R. Naranjo, DREAM is a Ca^{2+}-regulated transcriptional repressor, Nature 398 (1999) 80–84.
[26] M. Osawa, A. Dace, K.I. Tong, A. Valiveti, M. Ikura, J.B. Ames, Mg^{2+} and Ca^{2+} differentially regulate DNA binding and dimerization of DREAM, J. Biol. Chem. 280 (2005) 18008–18014.
[27] S. Huecas, C. Schaffner-Barbero, W. García, H. Yébenes, J.M. Palacios, J.F. Díaz, M. Menéndez, J.M. Andreu, The interactions of cell division protein FtsZ with guanine nucleotides, J. Biol. Chem. 282 (2007) 37515–37528.